14th European Signal Processing Conference (EUSIPCO 2006), Florence, Italy, September 4-8, 2006, copyright by EURASIP

RING BASED WAVELET TRANSFORM WITH ARBITRARY SUPPORTS IN WIRELESS SENSOR NETWORKS

Siwang Zhou[1]*, Yaping Lin*[2,1]*, and Yonghe Liu*[3]

[1] College of Computer and Communication, Hunan University, Changsha, China, 410082
[2] College of Software, Hunan University, Changsha, China, 410082
[3]Dept. of Computer Science and Engineering, The University of Texas at Arlington, Arlington, USA, TX 76019
E-mail: myswzhou@hotmail.com, yplin@hnu.cn, yonghe@cse.uta.edu

ABSTRACT

In this paper, we propose a general transform for wavelet based data compression in wireless sensor networks. By employing a ring topology, our transform is capable of supporting a broad scope of wavelets rather than specified ones. At the same time, the scheme is capable of simultaneously exploring the spatial and temporal correlations among the sensory data. Furthermore, the ring based topology is in particular effective in eliminating the "border effect" generally encountered by wavelet based schemes. Theoretically and experimentally, we show the proposed wavelet transform can effectively explore the spatial and temporal correlation in the sensory data and provide significant reduction in energy consumption compared to other schemes.

1. INTRODUCTION

Data compression has attracted extensive research efforts in wireless sensor networks targeting at reducing network load and hence energy consumption. In particular, a series of papers have pioneered in wavelet based distributed compression [1–4] recently. While these papers have provided certain insights in employing wavelet transform (WT), they are often limited to the discussion of a particular wavelet function with simple or special structures, notably among which is the Haar model. Although these algorithms are shown to be computationally simple, they often lack the generality required to be applied to a plethora of applications.

Furthermore, existing schemes have often focused on either exploiting the temporal correlation or spatial correlation of the sensory data, but not both. This, in turn has limited their performance and application scope.

Motivated thereby, in this paper, we propose a ring topology based distributed wavelet compression algorithm. Our scheme simultaneously exploits the spatial and temporal correlation residing in the sensory data within a cluster. Furthermore, our scheme is capable of accommodating a broad range of wavelets which can be designated by different applications. Moreover, the ring model will naturally eliminate the "border effects" encountered by WT and hence further strengthen its support to general wavelets. Theoretically and experimentally, we analyze the performance of the ring based WT and perform comparison with a non-distributed approach.

The remainder of this paper is organized as follows. In Section 2, we detail the ring model and describe the WT thereon. In Section 3, we analyze the performance of the proposed framework theoretically. Experimental study is presented in Section 4 and we conclude in Section 5.

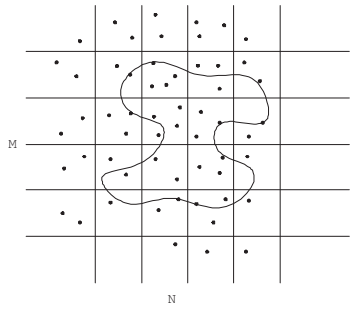

Figure 1: Ring topology based on virtual grid

2. SPATIAL-TEMPORAL WAVELET COMPRESSION ALGORITHM

In this section, we first present the network model and the construction of the virtual ring topology. The wavelet based algorithm for compressing spatial and temporal correlated data is then detailed.

2.1 Virtual Grid and Ring Topology

We assume that the sensor network is divided into different clusters, each of which is controlled by a cluster head [5]. Our focus is given to energy-efficient gathering of the sensory data from various cluster members to the cluster head. Routing the data from the cluster head to the sink is out of the scope of this paper although it may benefit from the compression algorithm presented in this paper. We assume that in each cluster, nodes are distributed in a virtual grid as illustrated in Fig. 1. Due to redundancy, one node in each grid cell is required to report its data to the cluster head. Without confusion, we will simply use node to refer to this reporting sensor. We remark that this model is neither restrictive nor unrealistic. In the worst case, a single node can be logically reside in one grid cell and can be required to report its data corresponding to every query or during every specified interval.

The key for our construction is that we form a ring topology among the reporting sensor nodes, as illustrated in Fig. 1. In this ring topology, neighboring nodes belong to spatial adjacent grid cells. A node on the ring receives data from one of its neighbors, fuses the data with its own, and further forward the results to the other neighbor. As the nodes are relaying the sensory data, WT will be executed and certain wavelet coefficients will be actually stored locally and some others will be forwarded. Indeed, nodes in a particular

grid cell can alternatively participate in the ring and hence the data gathering procedure. This way, energy consumption can be more evenly distributed among the nodes and thus extend the network lifetime. Readers are referred to [6] for approaches of scheduling nodes within one grid, for example, power on and off, for this purpose.

Given the ring topology, in each data gathering round, a node will be chosen as the "head" of the ring and the nodes will be indexed accordingly as $s_0, s_1, \cdots, s_i, \cdots, s_{N-1}$, where N is the number of nodes on the ring. In addition, we assume that sensor i stores data $c_{ji}, j = 0, 1, \cdots, M-1$, where j is the temporal index and c_{ji} represents the sensory data of sensor i at time index j. Evidently, dependent on M, each sensor will window out history data. Accordingly, we can arrange the sensory data on the ring according to their spatial and temporal relationship to a matrix $C^0 = \{c_{ji}\}, 0 \le i < N, 0 \le j < M$, where column i represents the data of sensor node i. For ease of notation, we will use $\vec{C}_i$ to denote column i. Notice that $\vec{C}_0$ and $\vec{C}_{N-1}$ are adjacent on the ring topology and hence will possess relatively higher correlation. As we will detail later, this unique feature of ring topology can effectively help us eliminate the border effects of WT.

2.2 Distributed Spatio-Temporal Wavelet Transform

Our goal is to employ the WT for compressing sensory data on the ring so that it can be energy efficiently transmitted to the cluster head. The approach is to simultaneously exploit the temporal and spatial correlation among the nodes' data and reduce the redundancy thereby. As the data is represented by matrix C^0, the temporal (within a node) and spatial (among multiple nodes) correlations are then captured by the columns and rows respectively. Correspondingly, in our design, we will first perform WT on each column and then perform WT on the rows. Furthermore, these column WT and row WT can be performed recursively to achieve a K-level WT. Notice that column WT is within a single node hence no communication is required although data shall be buffered. On the contrary, the row WT is among the sensor nodes and hence requires additional communications. Thereby, as will be discussed below, the scheme proposed by us will have many characteristics that are different with traditional 2-dimensional WT.

Our first step is to perform transform on the columns of C^0 to exploit temporal correlation. Let L_n and H_n be lowpass and highpass analysis filters respectively, we have

$$\begin{aligned} c^{1,L}_{m,i} &= \sum_n L_{(n-2m)} \vec{C}_i(n) \\ c^{1,H}_{m,i} &= \sum_n H_{(n-2m)} \vec{C}_i(n), \quad 0 \le m \le M/2-1 \end{aligned}$$

where $C^{1,L}_{m,i}$ represents the m^{th} approximation wavelet coefficient in i^{th} column in the first level of the column WT, $C^{1,H}_{m,i}$ is the corresponding detail wavelet coefficient, and $\vec{C}_i(n)$ denotes the n^{th} element of $\vec{C}_i$. Notice that this transform is performed within each node on its own sensory data and thus does not require any communication among the nodes on the ring. Subsequently, we can realign the resultant wavelet coefficients and obtain matrix C_1 as follow:

$$C_1 = \left\{ \begin{array}{cccc} c^{1,L}_{0,0} & c^{1,L}_{0,1} & \cdots & c^{1,L}_{0,N-1} \\ \vdots & \vdots & \ddots & \vdots \\ c^{1,L}_{\frac{M}{2}-1,0} & c^{1,L}_{\frac{M}{2}-1,1} & \cdots & c^{1,L}_{\frac{M}{2}-1,N-1} \\ c^{1,H}_{0,0} & c^{1,H}_{0,1} & \cdots & c^{1,H}_{0,N-1} \\ \vdots & \vdots & \ddots & \vdots \\ c^{1,H}_{\frac{M}{2}-1,0} & c^{1,H}_{\frac{M}{2}-1,1} & \cdots & c^{1,H}_{\frac{M}{2}-1,N-1} \end{array} \right\}$$

Given matric C_1, our second step is to perform WT on its rows to explore the spatial correlation among the nodes. Note that the first and the last column are adjacent on the ring topology, and this resembles a periodic extension to the signal. Towards this end, for general wavelets with arbitrary supports whose lowpass analysis filter is L_n, $-i_1 \le n < j_1$ and highpass analysis filter is H_n, $-i_2 \le n < j_2$, where $i_1, i_2, j_1, j_2 \ge 0$, we analyze the different cases of the row transform based on whether j_1 and j_2 are even or odd.

Case I: If j_1 is even and j_2 is odd, by performing WT on the rows in a similar way to the column WT, we obtain

$$C_2 = \left\{ \begin{array}{cccc} c^{1,LL}_{0,l_0} & c^{1,LH}_{0,h_0} & \cdots & c^{1,LL}_{0,l_{\frac{N}{2}-1}} & c^{1,LH}_{0,h_{\frac{N}{2}-1}} \\ \vdots & \vdots & \ddots & \vdots & \vdots \\ c^{1,LL}_{\frac{M}{2}-1,l_0} & c^{1,LH}_{\frac{M}{2}-1,h_0} & \cdots & c^{1,LL}_{\frac{M}{2}-1,l_{\frac{N}{2}-1}} & c^{1,LH}_{\frac{M}{2}-1,h_{\frac{N}{2}-1}} \\ c^{1,HL}_{0,l_0} & c^{1,HH}_{0,h_0} & \cdots & c^{1,HL}_{0,l_{\frac{N}{2}-1}} & c^{1,HH}_{0,h_{\frac{N}{2}-1}} \\ \vdots & \vdots & \ddots & \vdots & \vdots \\ c^{1,HL}_{\frac{M}{2}-1,l_0} & c^{1,HH}_{\frac{M}{2}-1,h_0} & \cdots & c^{1,HL}_{\frac{M}{2}-1,l_{\frac{N}{2}-1}} & c^{1,HH}_{\frac{M}{2}-1,h_{\frac{N}{2}-1}} \end{array} \right\}$$

where $l_i = (\frac{N-j_1+2i}{2} mod \frac{N}{2})$, $h_i = (\frac{N-j_2+2i+1}{2} mod \frac{N}{2})$, $c^{1,LL}_{m,l_i}$ and $c^{1,HL}_{m,l_i}$ represent the approximation coefficients in the first level of the row WT, and $c^{1,LH}_{m,h_i}$ and $c^{1,HH}_{m,h_i}$ represent the corresponding detail coefficients. We remark that for a node with index i, if i is even, the node stores coefficients $c^{1,LL}_{m,\frac{N-j_1+i}{2} mod \frac{N}{2}}$ and $c^{1,HL}_{m,\frac{N-j_1+i}{2} mod \frac{N}{2}}$; if i is odd, the node stores coefficients $c^{1,LH}_{m,\frac{N-j_2+i}{2} mod \frac{N}{2}}$ and $c^{1,HH}_{m,\frac{N-j_2+i}{2} mod \frac{N}{2}}$, $0 \le m \le M/2-1$. Notice that this transform is performed among the sensor nodes on the ring to harvest the spatial correlation and hence resultant wavelet coefficients cannot be realigned as in the column WT.

Based on the the approximation coefficients in C_2, we can obtain matrix C^1 as

$$C^1 = \left\{ \begin{array}{cccc} c^{1,LL}_{0,l_0} & c^{1,LL}_{0,l_1} & \cdots & c^{1,LL}_{0,l_{\frac{N}{2}-1}} \\ c^{1,LL}_{1,l_0} & c^{1,LL}_{1,l_1} & \cdots & c^{1,LL}_{1,l_{\frac{N}{2}-1}} \\ \vdots & \vdots & \ddots & \vdots \\ c^{1,LL}_{\frac{M}{2}-1,l_0} & c^{1,LL}_{\frac{M}{2}-1,l_1} & \cdots & c^{1,LL}_{\frac{M}{2}-1,l_{\frac{N}{2}-1}} \end{array} \right\}$$

We can perform the second level column and row WT on matrix C^1 as those to matrix C^0 and extend to K^{th} level spatio-temporal WT similarly.

Once the K-level WT is performed, the original data gathered by the nodes on the ring is transformed to the wavelet domain. Since the spatial and temporal correlations are exploited, we can represent the original data using fewer bits. In lossless compression, all the wavelet coefficients shall be encoded and sent to the cluster head; in lossy compression, according to different application-specific requirements, the wavelet coefficients can selectively encoded and sent to the cluster head by different nodes.

Case II: If j_1 and j_2 are both odd, while we can perform the transform following similar procedure, the matrices C_2 will be significantly different:

$$C_2 = \begin{Bmatrix} 0 & c_{0,l_0}^{1,LL}, c_{0,h_0}^{1,LH} & \cdots & 0 & c_{0,l_{\frac{N}{2}-1}}^{1,LL}, c_{0,h_{\frac{N}{2}-1}}^{1,LH} \\ \vdots & \vdots & \ddots & \vdots & \vdots \\ 0 & c_{\frac{M}{2}-1,l_0}^{1,LL}, c_{\frac{M}{2}-1,h_0}^{1,LH} & \cdots & 0 & c_{\frac{M}{2}-1,l_{\frac{N}{2}-1}}^{1,LL}, c_{\frac{M}{2}-1,h_{\frac{N}{2}-1}}^{1,LH} \\ 0 & c_{0,l_0}^{1,HL}, c_{0,h_0}^{1,HH} & \cdots & 0 & c_{0,l_{\frac{N}{2}-1}}^{1,HL}, c_{0,h_{\frac{N}{2}-1}}^{1,HH} \\ \vdots & \vdots & \ddots & \vdots & \vdots \\ 0 & c_{\frac{M}{2}-1,l_0}^{1,HL}, c_{\frac{M}{2}-1,h_0}^{1,HH} & \cdots & 0 & c_{\frac{M}{2}-1,l_{\frac{N}{2}-1}}^{1,HL}, c_{\frac{M}{2}-1,h_{\frac{N}{2}-1}}^{1,HH} \end{Bmatrix}$$

Note that those nodes whose indexes are odd will not store wavelet coefficients and become pure delays.

When j_1 is odd and j_2 is even, it will be similar to the first case, and when j_1 and j_2 are all even, it will be similar to the second case discussed above. i_1 and i_2 will not affect the distribution of wavelet coefficients. The reason is that when we perform row WT, the first group of approximation coefficients are calculated using the data stored in the $((N - i_1)modN)^{th}$ node to the $(j_1 modN)^{th}$ node and are stored in the $(j_1 modN)^{th}$ node. The corresponding detail coefficients are calculated using the data stored in the $(N - i_2)^{th}$ node to the $(j_2 modN)^{th}$ node and are stored in the $(j_2 modN)^{th}$ node.

2.3 An Example based on D4 Wavelet

An advantage of the above scheme is its support of general wavelets. Here, using D4 wavelet [7] as an example, we illustrate the operation of the described scheme. Considering a ring of N=8 nodes as illustrated in Fig. 2 where s_0 is the ring head. Let M=8. According to our design, node s_i shall store data vector $\vec{C}_i = [c_{0i}\ c_{1i}\ \cdots\ c_{7i}]^T$. Let the lowpass analysis filter of D4 be L_n, where $0 \le n \le 3$, and the highpass analysis filter be H_n, where $-1 \le n \le 2$. A 2-level distributed spatio-temporal WT based on D4 is shown in Fig. 2.

Note that all the nodes shall store wavelet coefficients as

$s_0 : c_{0,3}^{1,LH}, \cdots, c_{3,3}^{1,LH}, c_{0,3}^{1,HH}, \cdots, c_{3,3}^{1,HH}$,
$s_1 : c_{0,3}^{1,HL}, \cdots, c_{3,3}^{1,HL}, c_{0,0}^{2,HL}, c_{1,0}^{2,HL}, c_{0,0}^{2,LL}, c_{1,0}^{2,LL}$,
$s_2 : c_{0,0}^{1,LH}, \cdots, c_{3,0}^{1,LH}, c_{0,0}^{1,HH}, \cdots c_{3,0}^{1,HH}$,
$s_3 : c_{0,0}^{1,HL}, \cdots, c_{3,0}^{1,HL}, c_{0,1}^{2,LH}, c_{1,1}^{2,LH}, c_{0,1}^{2,HH}, c_{1,1}^{2,HH}$,
$s_4 : c_{0,1}^{1,LH}, \cdots, c_{3,1}^{1,LH}, c_{0,1}^{1,HH}, \cdots, c_{3,1}^{1,HH}$,
$s_5 : c_{0,1}^{1,HL}, \cdots, c_{3,1}^{1,HL}, c_{0,1}^{2,HL}, c_{1,1}^{2,HL}, c_{0,1}^{2,LL}, c_{1,1}^{2,LL}$,
$s_6 : c_{0,2}^{1,LH}, \cdots, c_{3,2}^{1,LH}, c_{0,2}^{1,HH}, \cdots, c_{3,2}^{1,HH}$,

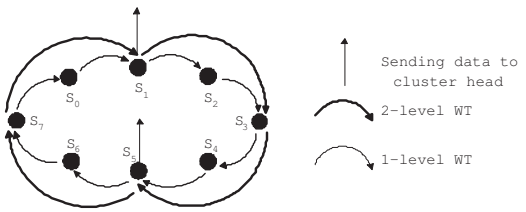

Figure 2: An Illustration Using D4 Wavelet

$s_7 : c_{0,2}^{1,HL}, \cdots, c_{3,2}^{1,HL}, c_{0,0}^{2,LH}, c_{1,0}^{2,LH}, c_{0,0}^{2,HH}, c_{1,0}^{2,HH}$.

As s_0 is the ring head, if we only need approximation coefficients to do lossy compression, nodes s_1 and s_5 shall send data to the cluster head, as illustrated in Fig. 2. Instead, if s_1 is selected as the ring head, the nodes that shall send data to the cluster head shall be s_2 and s_6.

2.4 Discussion

In the above WT, the ring head can be alternated among different nodes when performing the data gathering procedure. Consequently, the wavelet coefficients will be distributed to different nodes accordingly which in turn will balance the energy consumption within the cluster. Furthermore, neighboring nodes on the ring belong to spatial adjacent virtual grids, so the data gathered by the neighboring nodes are more likely spatially correlated. Because the calculation of approximation and detail wavelet coefficients are for neighboring nodes within a support length, performing WT based on the ring can make full use of spatial correlation to remove the data redundancy and hence reduce transmission cost.

More importantly, performing WT based on ring topology naturally eliminates the "border effect" problem inherent in WT. It is well known that general wavelet functions are defined on the real axis $\Re$ while the signal is always limited in a finite region $\aleph$. Therefore, the approximate space $L^2(\Re)$ will not match the signal space $L^2(\aleph)$ which will result in the "border effect" [8] and thus introduce errors during signal reconstruction. For example, for the famous Daubechies wavelet with supports 7, if three-level WT are performed in the cluster that consists of 128 sensor nodes and the "border effect" is not considered, fraction of number of nodes with false reconstructed value to that of total nodes will reach 58 percent. Along with the increasing levels of WT, the "border effect" will be more remarkable and hence more nodes will be affected. One of the general methods to deal with "border effect" is extending border. The ring topology resembles a periodic extension to the signal that naturally dissolves the "border effect".

3. ANALYSIS

We now briefly analyze the energy consumption and delay of the proposed scheme. For this purpose, we adopt the first order radio model described in [5]. In this model, a radio dissipates E_{elec} amount of energy at the transmitter or receiver circuitry and ε_{amp} amount of energy for transmit amplifier. Signal attenuation is modeled to proportional to d^2 on the channel, where d denotes distance. For k bits data and a distance d, the transmission energy consumption E_{Tx} and recep-

tion energy consumption E_{Rx} can be calculated respectively as

$$\begin{aligned} E_{Tx}(k,d) &= E_{Tx-elec}(k)+E_{Tx-amp}(k,d) \\ E_{Tx}(k,d) &= E_{elec}k+\varepsilon_{amp}\cdot k\cdot d^2 \\ E_{Rx}(k) &= E_{Rx-elec}(k)=E_{elec}\cdot k \end{aligned}$$

We further assume that the sensor nodes can transmit simultaneously and neglect the processing and propagation delay. Let the transmission time of one data unit be one unit time. Let E_{IN} and D_{IN} represent the energy consumption and delay resulting from communication among the nodes within the cluster for performing the proposed WT. We can derive the following theorem.

Theorem 1: For general wavelets with arbitrary supports, let the lowpass analysis filter be $L_n, -i_1 \le n < j_1$, and the highpass analysis filter be $H_n, -i_2 \le n < j_2$, where $i_1, i_2, j_1, j_2 \ge 0$. For a K-level distributed spatio-temporal WT based on the ring topology proposed above, to gather the sensory data in a cluster of N node, we have

$$\begin{aligned} E_{IN} &= \sum_{n=1}^{K}\sum_{l=0}^{N/2^n-1}(E_{n,l}^P+2E_{elec}(\sum_{i=0}^{i_1+j_1+1}q_{inl}^L+\sum_{i=0}^{i_2+j_2+1}q_{inl}^H) \\ &\quad +\varepsilon_{amp}(\sum_{i=0}^{i_1+j_1+1}(q_{inl}^L\cdot d_{inl}^L)+\sum_{i=0}^{i_2+j_2+1}(q_{inl}^H\cdot d_{inl}^H))) \quad (1) \\ D_{IN} &= \sum_{n=1}^{K}(\max_{0\le l\le \frac{N}{2^n}-1}(\sum_{i=0}^{i_1+j_1-1}q_{inl}^L) \\ &\quad +\max_{0\le l\le \frac{N}{2^n}-1}(\sum_{i=0}^{i_2+j_2-1}q_{inl}^H)) \quad (2) \end{aligned}$$

where

$$\begin{aligned} q_{inl}^L &= q_{n,(-i_1+N+2^nl+(2^{n-1}-1)(i_1+j_1)+2^{n-1}i)modN}^L, \\ q_{inl}^H &= q_{n,(-i_2+N+2^nl+(2^{n-1}-1)(i_2+j_2)+2^{n-1}i)modN}^H, \\ d_{inl}^L &= (\sum_{j=-i_1+N+2^nl+(2^{n-1}-1)(i_1+j_1)}^{-i_1+N+2^nl+(2^{n-1}-1)(i_1+j_1)+2^{n-1}-1}d_{jmodN})^2, \\ d_{inl}^H &= (\sum_{j=-i_2+N+2^nl+(2^{n-1}-1)(i_2+j_2)}^{-i_2+N+2^nl+(2^{n-1}-1)(i_2+j_2)+2^{n-1}-1}d_{jmodN})^2, \end{aligned}$$

q_{inl}^L and q_{inl}^H are the data amount transmitted by the i^{th} node when the l^{th} approximation coefficient and the corresponding detail coefficient in the n^{th} level row WT are calculated respectively, d_{jmodN} is the distance between the $(jmodN)^{th}$ node and the $((j+1)modN)^{th}$ node, $E_{n,l}^P$ is the processing energy of when the l^{th} wavelet coefficients is calculated in the n^{th} level WT.

Proof: When the l^{th} approximation wavelet coefficient in the n^{th} level row WT is calculated, the transmitting cost $E_{n,l}^L$ is: $E_{n,l}^L = E_{Tx}+E_{Rx} = 2E_{elec}\sum_{i=0}^{i_1+j_1}q_{inl}^L+\varepsilon_{amp}\sum_{i=0}^{i_1+j_1}(q_{inl}^L\cdot d_{inl}^L)$ (3). When the l^{th} detail wavelet coefficient in the n^{th} level row WT is calculated, the transmitting cost $E_{n,l}^H$ is: $E_{n,l}^H = 2E_{elec}\sum_{i=0}^{i_2+j_2}q_{inl}^H+\varepsilon_{amp}\sum_{i=0}^{i_2+j_2}(q_{inl}^H\cdot d_{inl}^H)$ (4). When the n^{th} level WT is performed, the processing cost E_p is: $E_P = \sum_{l=0}^{\frac{N}{2^n}-1}E_{n,l}^P$ (5). Then, the energy consumption in the n^{th} WT is $E_{n,IN}$: $E_{n,IN} = E_P+\sum_{l=0}^{N/2^n-1}(E_{n,l}^L+E_{n,l}^H)$ (6). If K-level WT are performed, the energy cost E_{IN} is: $E_{IN} = \sum_{n=1}^{K}(E_p+\sum_{l=0}^{\frac{N}{2^n}-1}(E_{n,l}^L+E_{n,l}^H))$ (7). Taking (3), (4) and (5) into (7), we can obtain (1). The network delay of the n^{th} WT is $D_{n,IN}$: $D_{n,IN} = \max_{0\le l\le\frac{N}{2^n}-1}(\sum_{l=0}^{i_1+j_1-1}q_{inl}^L)+\max_{0\le l\le\frac{N}{2^n}-1}(\sum_{l=0}^{i_2+j_2-1}q_{inl}^H)$ (8). Hereby, it is easy to get (2).

Notice that $E_{n,l}^P$ includes two parts: one is the processing cost when nodes perform column WT in single node, the other is the processing cost when nodes fuse data obtained from the proceeding nodes. We can conclude from the theorem that, along with increasing levels of the WT, the energy cost also increases. However, the detail wavelet coefficients stored by the nodes also increase. As a result, the data can be coded using fewer bits.

For performance comparison, we employ a *non-distributed approach* for data gathering. In this approach, sensor nodes in the cluster will send their data to the cluster head directly and thus no inter-nodes communications are required. Comparing the energy consumption and delay between our algorithm and the non-distributed approach, we have the following theorem.

Theorem 2: Let the average distance between nodes and the cluster head be D meters. Let the amount of the original data that is quantized be Q bits and the amount of data be Q' bits after K-level distributed spatio-temporal WT is performed. We have 1) If $Q' \le Q - E_{IN}/(E_{elec}+\varepsilon_{amp}\cdot D^2)$, the energy consumption by performing our algorithm is less than that of non-distributed approach; 2) If $Q' \le Q - D_{IN}$, the delay by performing our algorithm is smaller than that of the non-distributed approach.

We omit the proof but note that the ratio of the total energy consumption of our algorithm and that of the non-distributed approach is

$$\frac{E_D}{E_C} = \frac{E_{IN}+E_{elec}Q'+\varepsilon_{amp}Q'D^2}{E_{elec}Q+\varepsilon_{amp}QD^2} = \frac{E_{IN}}{E_{elec}Q+\varepsilon_{amp}QD^2}+\frac{Q'}{Q}$$

Evidently, E_D/E_C will decrease when the distance D increase. Therefore, we can conclude that with increasing distance between the cluster members from the cluster head, the proposed algorithm will save more energy.

4. SIMULATION AND RESULTS

In this section, using Haar wavelet we evaluate the performance of our algorithm and in particular compare it with the non-distributed approach.

We consider a ring composed of 100 nodes, assuming that the nodes are uniformly distributed and the average distance among the neighboring nodes is 5 meters. We use real life data obtained from the Tropical Atmosphere Ocean Project (http://www.pmel.noaa.gov/tao/), which is the ocean temperatures sampled by 100 sensor nodes on different mornings at different depths at 12:00pm from 1/20/2004 to 5/26/2004. In the experiment, we employ uniform quantization and no entropy coding. Three cases are compared:

1-level Haar, 2-level Haar, and the aforementioned non-distributed approach. For the energy consumption model, we use $E_{elec} = 50nJ/bit$ and $\varepsilon_{amp} = 100pJ/bit/m^2$. The results are shown in Fig. 3 to Fig. 5. Fig. 3 and Fig. 4 illustrate the the relation among the distance D between nodes and cluster head, the peak-value signal to noise ratio *PSNR*, and the energy cost E_D and delay D_D for 1-level Haar and 2-level Haar. Fig. 5 summarizes the results for the non-distributed approach.

As we can see, when the fraction of the discarding detail coefficients to the total wavelet coefficients in the 1-level and 2-level WT reaches 59 percents and 68 percents respectively, the *PSNR* still remains 61dB. The reason is that the data used in the simulation have strong spatio-temporal correlation and our proposed algorithm can can exploit them efficiently. At the same time, the energy consumption for communication among the nodes of 1-level WT is smaller than that of 2-level. Note that the non-distributed approach does not incur energy consumption for communications among the nodes on the ring. However, seen in our simulation, when the distance between the nodes and the cluster head is larger than 40 meters, even if PSNR reaches 61dB which is well above general system requirements, the total energy consumption of the non-distributed approach is still larger than that of 1-level WT, which in turn is larger than that of 2-level WT. This indicates that the benefit of compression outweighs the energy due to inter-node communication for performing the WT. This actually testifies for the conclusion drawn in Theorem 2. At the same time, for the same *PSNR*, the delay of 2-level distributed spatio-temporal is smaller than that of 1-level, which in turn is smaller than that of the non-distributed approach. This also concurs with Theorem 2.

5. CONCLUSION

In this paper, we have proposed a distributed spatio-temporal compression algorithm based on the ring model for general wavelets with arbitrary supports. In particular, our algorithm can accommodate a broad range of wavelet functions in order to effectively exploit the temporal and spatial correlation for data compression. Furthermore, the ring topology can effectively eliminate the "border effect" by naturally extending the signal space. Our theoretical and experimental results show that the proposed scheme can achieve significant reduction in energy consumption and delay for data gathering in a sensor cluster.

We are currently investigating the methods to effectively accept or reject the detail wavelet coefficients generated by the scheme so that constant or limited bit rate for sensor transmission can be achieved.

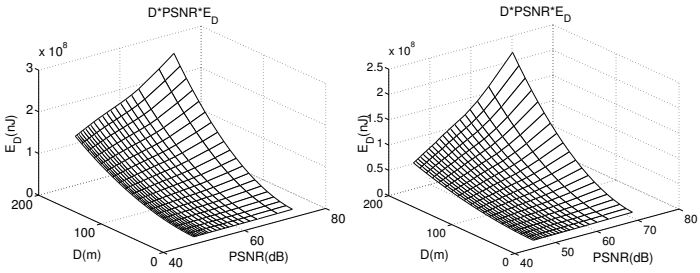

(a) For 1-level WT (b) For 2-level WT

Figure 3: $PSNR \times E_D \times D$ for WT

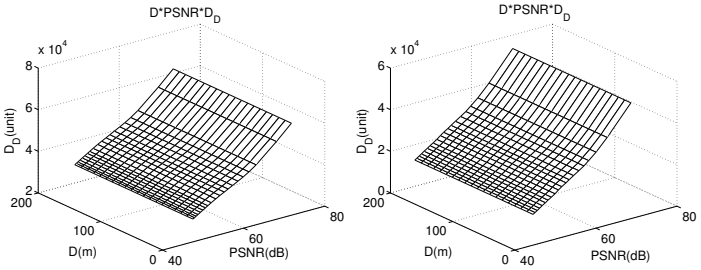

(a) For 1-level WT (b) For 2-level WT

Figure 4: $PSNR \times D_D \times D$ for WT

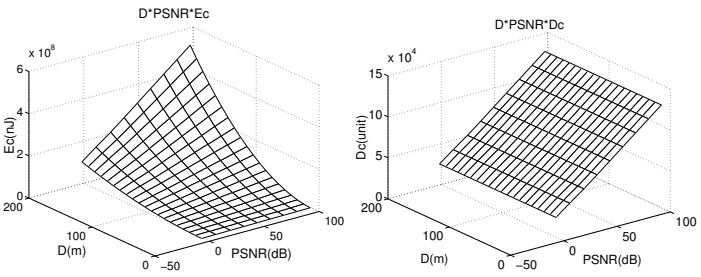

(a) $PSNR \times E_C \times D$ (b) $PSNR \times D_C \times D$

Figure 5: Non-distributed Approach

REFERENCES

[1] A. Ciancio and A. Ortega, "A distributed wavelet compression algorithm for wireless sensor networks using lifting," in *Proc. ICASSP*, Montreal, Canada, May 2004.

[2] J. Acimovic, R. Cristescu and B. Lozano, "Efficient distributed multiresolution processing for data gathering in sensor networks," in *Proc. ICASSP*, Philadelphia, USA, March 2005.

[3] R. Cristescu, B. Lozano, M. Vetterli, D. Ganesan, and J. Acimovic, "On the interaction of data representation and routing in sensor networks," in *Proc. ICASSP*, Philadelphia, USA, March 2005.

[4] R. Wagner, S. Sarvotham, and R. Baraniuk, "A multiscale data representation for distributed sensor networks," in *Proc. ICASSP*, Philadelphia, USA, March 2005.

[5] W. Heinzelman, A. Chandrakasan, and H. Balakrishnan,"Energy-Efficient Communication Protocol for Wireless Microsensor Networks," in *Proc. HICSS*, Hawaii, USA, January 2000.

[6] Y. Xu, J. Heidemann, and D. Estrin,"Geography-informed energy conservation for ad hoc routing," in *Proc. MobiCom*, Rome, Italy, July 2001.

[7] I. Daubechies," Orthonormal bases of compactly supported wavelets",*Comm. Pure applied Math.*, vol. 41, pp. 909-996, 1988.

[8] G. Karlsson and M. Vetterli," Extension of finite length signals for subband coding,"*Signal processing*, vol.17, pp.161-168, 1989.